Electronic Supplementary Material (ESI) for Green Chemistry.

Supplementary information:

Towards low carbon process for lithium recovery from spent lithium-ion batteries by carbon conversion control strategy of carbothermic reduction

Yue Wang [a, b], Xiaohong Zheng [b, c], Weiguang Lv [b], Li Li[a], Zhi Sun [b]

[a] School of Materials Science & Engineering, Beijing Institute of Technology, Beijing 100081,China.

[b] Beijing Engineering Research Center of Process Pollution Control, Key Laboratory of Green Process and Engineering, Division of Environment Technology and Engineering, Institute of Process Engineering, Chinese Academy of Sciences, Beijing 100190, China

[c] Beijing Key Laboratory of Materials Utilization of Nonmetallic Minerals and Solid Wastes, National Laboratory of Mineral Materials, School of Materials Science and Technology, China University of Geosciences (Beijing), Beijing 100083, China.

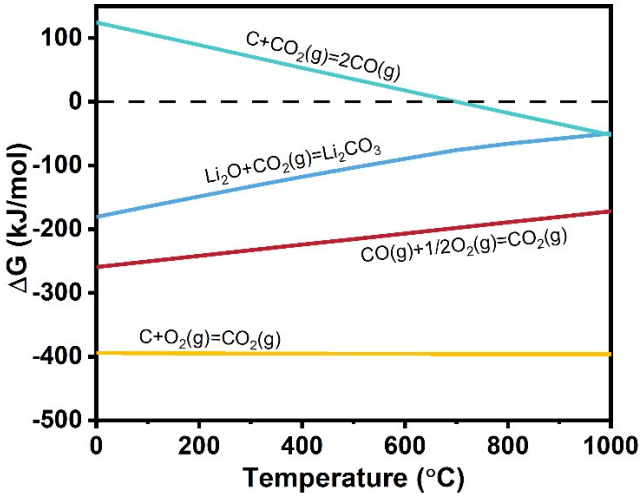

Fig. S1 Gibbs free energy values (ΔG) of possible thermodynamic reactions during heating from 0℃~1000℃

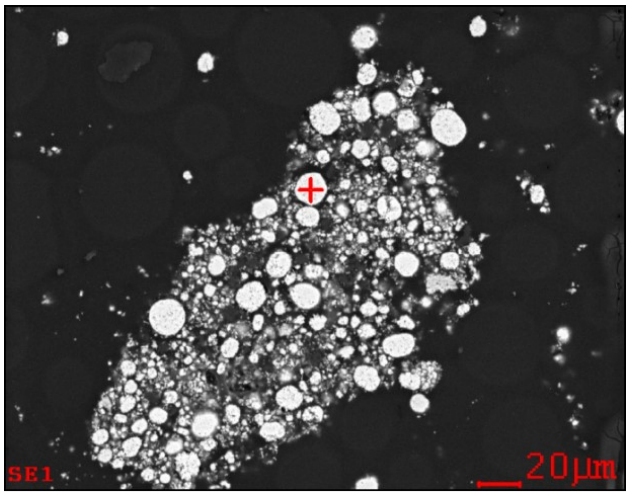

Fig.S2 Cross-sectional SEM image of intermediate roasted product

Table S1. The distribution of elements at the tag in Fig.S2

Element	Wt%	At%
O	31.76	46.72
Mn	15.90	6.81
Co	15.56	6.32
Ni	29.93	12.14

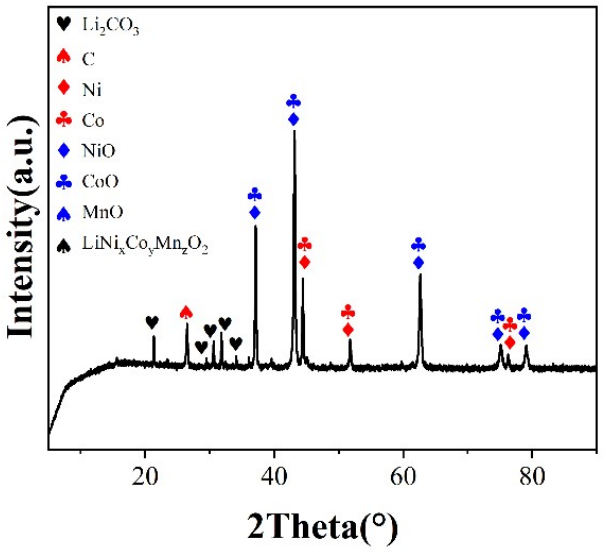

Fig.S3 XRD pattern of incompletely roasting product

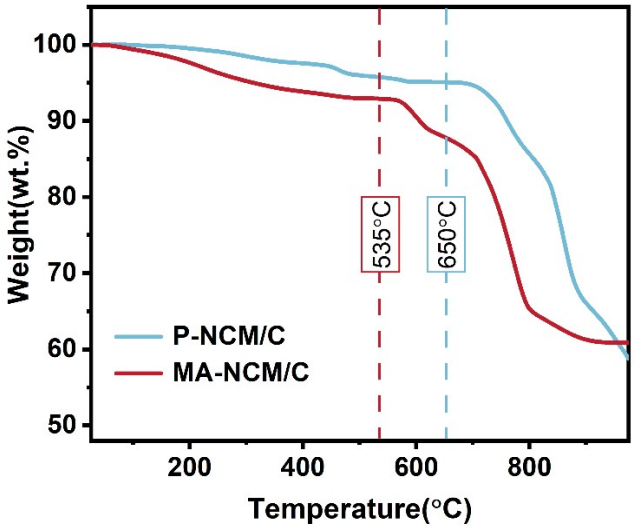

Fig S4 Thermogravimetry (TG) curves of the untreated and activated mixing powders ($LiNi_{0.5}Co_{0.2}Mn_{0.3}O_2$: graphite = 6:1, rotating time = 6 h, rotating speed = 600 rpm/min, and ball-to-powder mass ratio = 20:1) during the heating process

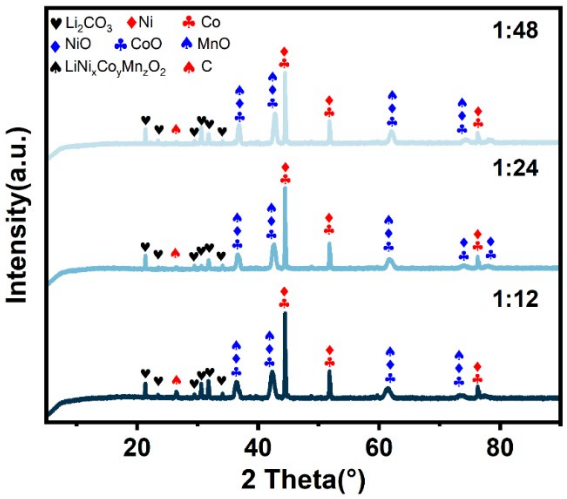

Fig S5 XRD results of the non-activated roasting products at different carbon dosages

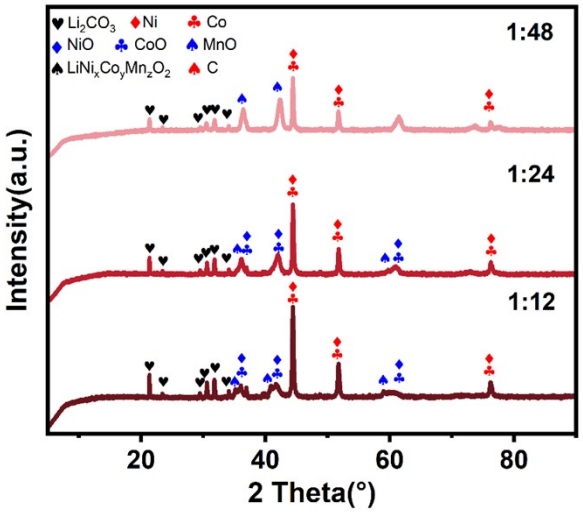

Fig S6 XRD results of the activated roasting products at different carbon dosages

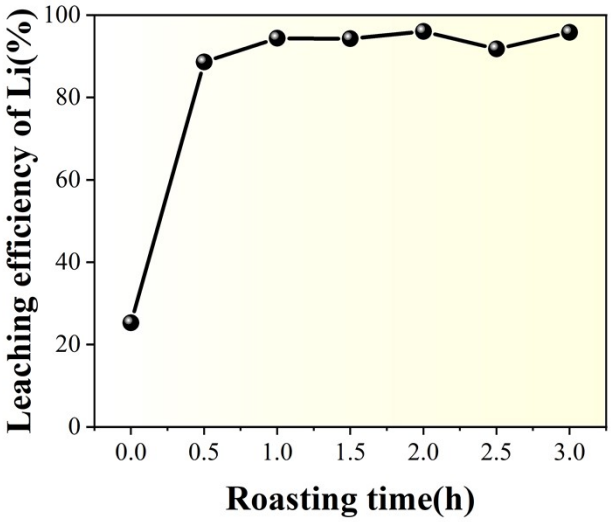

Fig S7 Leaching efficiency of Li on the conditions of different roasting time

As depicted in Fig.S7, when the roasting time is further increased to 1 h or longer, the leaching efficiency of Li is higher than 95%; therefore, the optimal roasting time is 1 h. Notably, the leaching efficiency of Li exceeded by 20% when the sample underwent mechanochemical activation without roasting prior to water leaching. This implies that the pre-reactions between the cathode and graphite might be triggered under the action of the mechanical force.

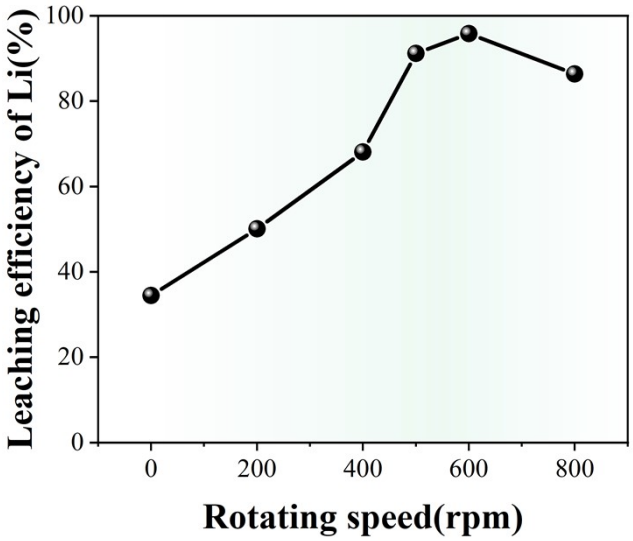

Fig S8 Leaching efficiency of Li on the conditions of different roasting speed.

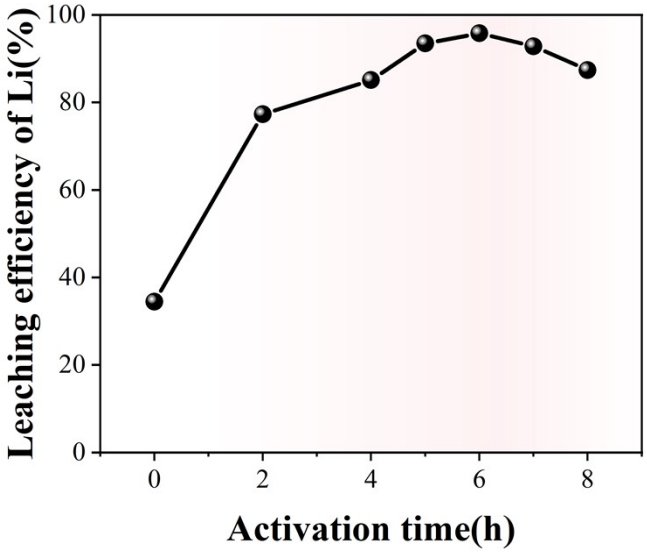

Fig S9 Leaching efficiency of Li on the conditions of different activation time.

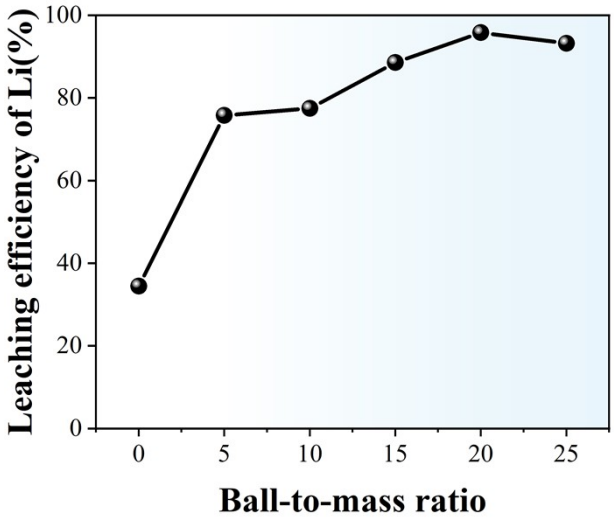

Fig S10 Leaching efficiency of Li on the conditions of different ball-to-mass ratio.

Figs.S8−10 show the influences of the activation parameters including rotation time, rotation speed, and ball-to-powder mass ratio on the leaching efficiency of Li. With increasing rotation time, rotation speed, and ball-to-powder mass ratio, the leaching ratios of Li in both untreated and activated products increased at the beginning and then decreased; moreover, no leaching of Ni, Co, and Mn were detected. For an activation time of 6 h, the rotation speed of 600 rpm/min, and ball-to-powder mass ratio of 20, the maximum leaching efficiency of Li was 95.78%.

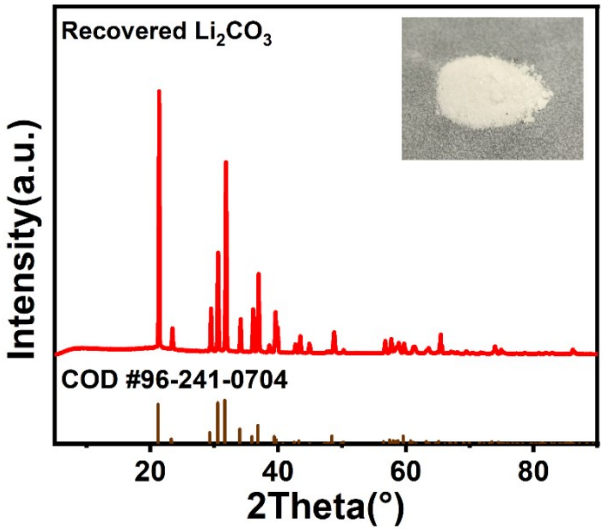

Fig.S11 XRD pattern of recovered Li_2CO_3

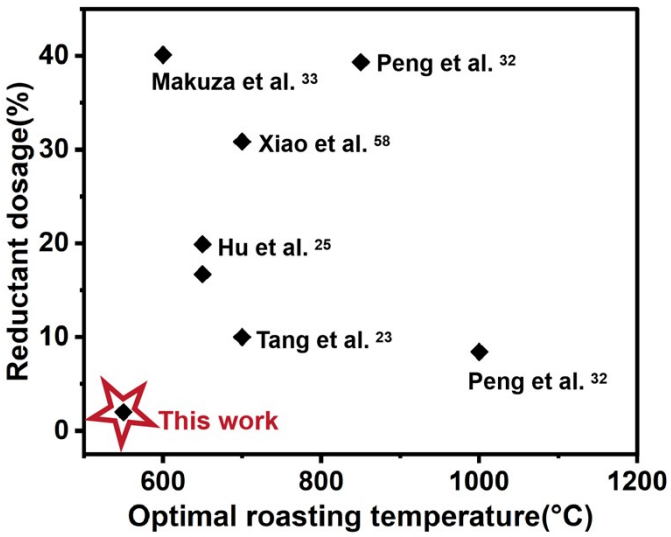

Fig. S12 Comparison between this work and previous work.

Table S2. Possible reaction paths between C and $LiCoO_2$

Reactants	**C**	**$LiCoO_2$**	**Li_2O**	**CoO**	**Co**	**CO_2**	**CO**
Amount of substance	0.25	1	0.5	1		0.25	
	0.75	1	0.5		1	0.5	
	0.5	1	0.5	1			0.75
	1.5	1	0.5		1		1.5

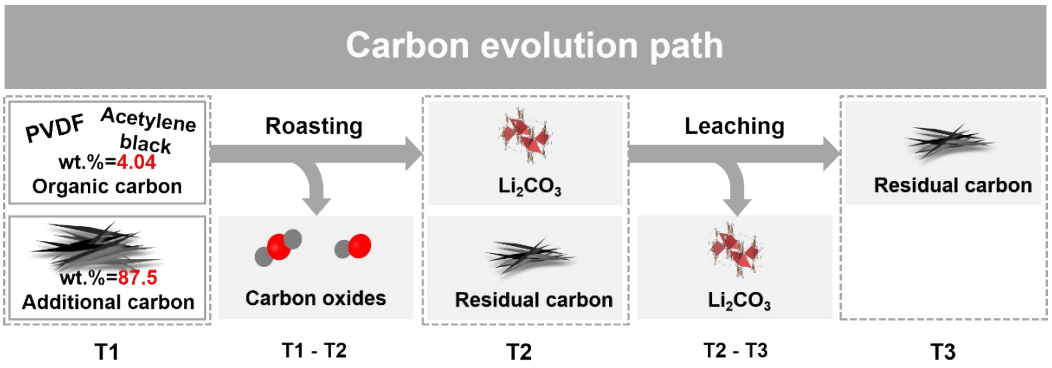

Fig. S13 Schematic diagram of the carbon evolution path in the roasting process.

Table S3. The carbon content of each stage in the roasting process

	Carbon Dosage	Total Mass/g	T1/g	(T1-T2)/g	T2/g	(T2-T3)/g	T3/g
P-NCM/C	**12:1**	1.3043	0.1389	0.0308	0.1081	0.0553	0.0528
	24:1	1.2532	0.0927	0.0045	0.0882	0.0506	0.0376
	48:1	1.2302	0.0712	0.0004	0.0708	0.0472	0.0236
MA-NCM/C	**12:1**	1.2094	0.1222	0.0204	0.1018	0.0613	0.0468
	24:1	1.1303	0.0834	0.0022	0.0812	0.0573	0.0239
	48:1	1.1812	0.0680	0.0004	0.0676	0.0583	0.0093

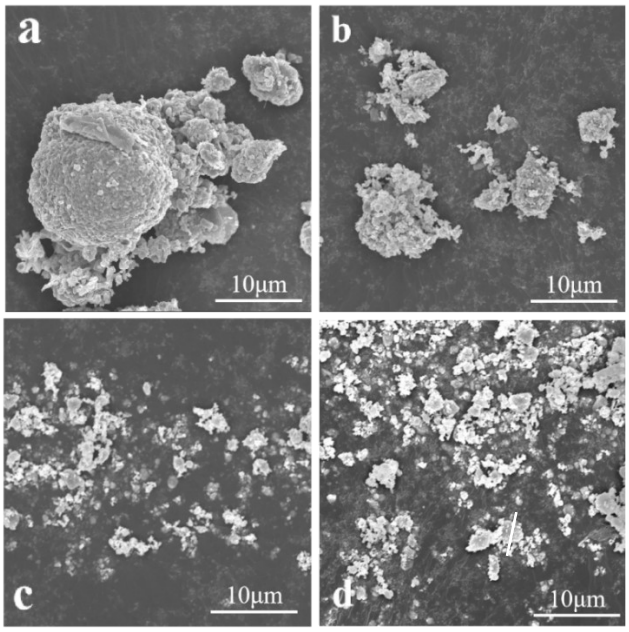

Fig.S14 SEM images of MA-NCM/C (a)0h, (b)2h, (c)4h and (d)6h

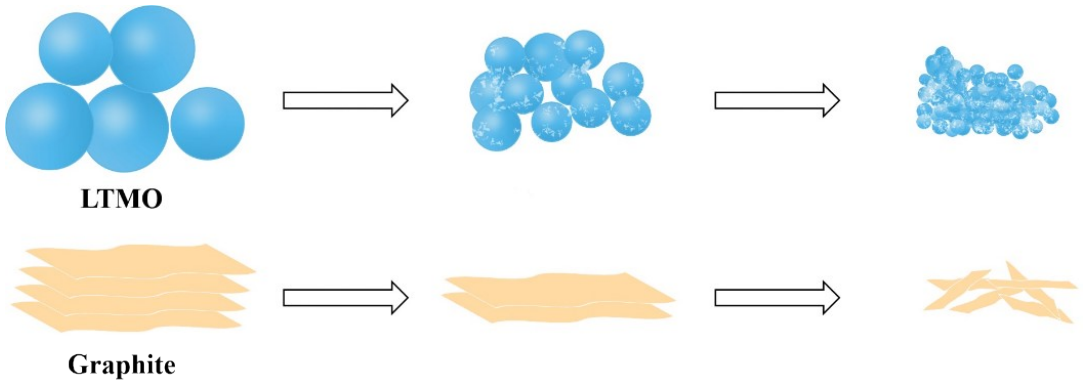

Fig.S15 Diagram of morphology change of the cathode and graphite during mechanochemical activation

Table S4. Fitting peaks of the O1s XPS spectra of the mixed samples activated at different rotation time

Samples	O_{latt}		O_{sur}		O_{sur}/O_{latt}
	Area	Position	Area	Position	
0h	29.54%	529.13 eV	70.46%	531.46 eV	2.38
2h	24.62%	529.34 eV	75.38%	531.49 eV	3.06
4h	23.43%	529.30 eV	76.57%	531.39 eV	3.26
6h	20.21%	529.33 eV	79.79%	531.47 eV	3.95

The data of the fitting peaks of the O1s XPS spectra was calculated by the XPS peak software.

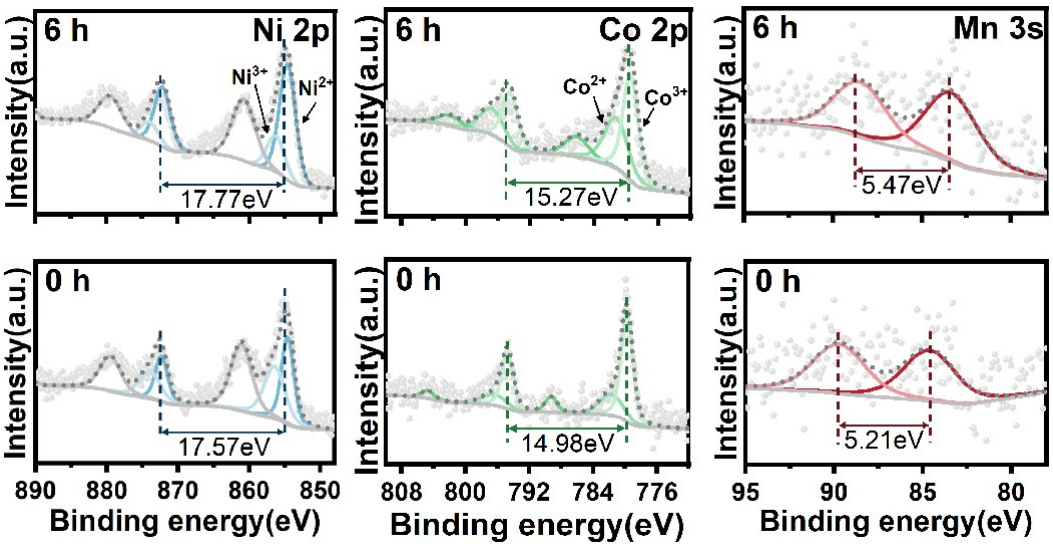

Fig.S16 High-resolution XPS spectrums of Ni 2p, Co 2p and Mn 2p in the MA-NCM activated under 0h and 6h

The Ni 2p spectrum reveals that Ni^{2+} and Ni^{3+} are present in the MA-NCM/C and the percentages of Ni^{2+} and Ni^{3+} could be obtained by analysing the Ni $2p_{3/2}$ spectrum, in which the peak located at 854.8 eV was attributed to Ni^{2+} and that at 856.8 eV to Ni^{3+} [1].

In the Co 2p high-resolution spectrum, the core peak is also split into two main peaks, which ascribed to Co $2p_{3/2}$ and Co $2p_{1/2}$ [2]. And when the activation time extended, the peak area of Co^{3+} which located at 779.8eV[3] shrinks inversely to the variation of activation time.

References:

1. Y. Shen, H. Xue, S. Wang, D. Zhang, D. Yin, L. Wang and Y. Cheng, *Chem. Eng. J.*, 2021, **411**.
2. L. Dahéron, R. Dedryvère, H. Martinez, M. Ménétrier, C. Denage, C. Delmas and D. Gonbeau, *Chemistry of Materials*, 2008, **20**, 583-590.
3. E. J. Van, J. L. Wieland, H. Eskes, P. Kuiper and T. S. Turner, *J Physical review. B, Condensed matter*, 1991, **44**, 6090-6103.